Color Invariant Snakes

Theo Gevers, Sennay Ghebreab and Arnold W.M. Smeulders
ISIS, University of Amsterdam, Kruislaan 403
1098 SJ Amsterdam, The Netherlands
{gevers, ghebreab, smeulders}@wins.uva.nl

Abstract

Snakes provide high-level information in the form of continuity constraints and minimum energy constraints related to the contour shape and image features. These image features are usually based on intensity edges. However, intensity edges may appear in the scene without a material/color transition to support it. As a consequence, when using intensity edges as image features, the image segmentation results obtained by snakes may be negatively affected by the imaging-process (e.g. shadows, shading and highlights).

In this paper, we aim at using color *invariant* gradient information to guide the deformation process to obtain snake boundaries which correspond to material boundaries in images discounting the disturbing influences of surface orientation, illumination, shadows and highlights.

Experiments conducted on various color images show that the proposed color invariant snake successfully find material contours discounting other "accidental" edges types (e.g. shadows, shading and highlight transitions). Comparison with intensity-based snakes shows that the intensity-based snake is dramatically outperformed by the presented color invariant snake.

1 Introduction

Active contour models can assist the process of image segmentation by providing high-level information in the form of continuity constraints and minimum energy constraints related to the contour shape and image characteristics. The active contour method that has attracted most attention is known as snake [4], for example. A snake is an energy minimizing curve which deforms its shape under the control of internal and external forces. These forces are specified so that the snake will hopefully achieve a minimal energy state when it matches the desired boundary to be detected. Snakes are used in many applications, including shape modeling, interactive image segmentation and motion tracking. In this paper, we focus on using snakes for interactive image segmentation.

In general, snakes use image features which are based on intensity gradient information. However, intensity edges or region outlines may appear in the scene without a material transition to support it. For example, the intensity of solid objects varies with object shape yielding prominent intensity edges when the orientation of the surface changes abruptly. In addition, the intensity of the illumination may vary spatially over the scene causing a gradual change in intensity over the object's surface even though the surface is homogeneously painted. Moreover, intensity boundaries can be caused by shadows and highlights. It is our point of view that image segmentation methods should rely on the change of material only, discounting the disturbing influences of surface orientation change, illumination, shadows and highlights.

Because intensity-based edge detectors cannot distinguish between various transition types, our attention is directed towards the use of color information. The choice of color features is of great importance for the purpose of proper image segmentation. It induces the equivalence classes to the actual segmentation algorithm. The choice which color features to use depends on the imaging conditions. It is well known that the RGB values obtained by a color camera will be negatively affected (color values will shift in RGB-color space) by the image-forming process [2], [3], for example. Therefore, in this paper, a snake-based image segmentation method is proposed on the basis of physics considerations leading to image features which are robust to the imaging conditions. To this end, various well-known color features are studied for the dichromatic reflection model. Then, color features are selected enabling the snake algorithm to converge to object contours corresponding to material boundaries in images discounting the disturbing influences of surface orientation, illumination, shadows and highlights. The novelty of this work is not to propose a new snake model but to use color *invariant* gradient information (in a standard snake model) instead of using intensity gradient information steering the deformation process.

To evaluate the performance of the color invariant snake with respect to intensity-based snakes, experiments have been conducted on color images taken from full-color objects in real-world scenes where objects are composed of a large variety of materials including plastic, textile, paper, wood, rubber, painted metal, ceramic and fruit. In addition, the images show a considerable amount of noise, shadows, shading, inter-reflections and specularities.

The paper is organized as follows. In Section 2, we review the properties and behavior of snakes. In Section 3, we propose robust color invariant gradients on which the color snake is based. Finally, experiments are conducted on various color images.

2 Active Contour Methods: Snakes

An active contour is a deformable (continuous) curve

$$\mathbf{v}(t) = [x(t), y(t)], t \in [0, 1] \tag{1}$$

that moves through the spatial domain of an image I to minimize an energy functional E. The energy E associated with the curve is a weighted sum of internal and external energies

$$E = \alpha E_{int} + \beta E_{ext} \tag{2}$$

The advantages of active contour methods can be summed as follows: (1) it is tolerant to noise (due to the integration of the energy values over the entire contour), (2) it enables inclusion of a priori knowledge (therefore it is tolerant to ambiguities in images such as gaps), (3) it provides an intuitive interaction mechanism, and (4) it is well suited for motion tracking. In order to illustrate the basic principles, which are the same for most snake methods, we will briefly discuss them.

The internal energy of a snake measures the desired properties of a contour's shape. In order to obtain smooth and physically feasible results, an elasticity and smoothness constraint are used in the energy functional. The smoothness constraint is, in general, based on the curvature of the active contour, which may be computed analytically from the properties of the contour. Then the internal energy is defined as follows:

$$E_{int} = (\oint_t (|\mathbf{v}(t)'||^2 + ||\mathbf{v}(t)''||^2 dt)(\oint_t ||\mathbf{v}(t)'||dt) \quad (3)$$

where $\mathbf{v}(t)'$ and $\mathbf{v}(t)''$ denote the first and second derivative of the curve with respect to t, and are measures for respectively the elasticity and smoothness. Measures independent of the spatial scale are obtained by multiplying the shape measure with the length of the contour.

The external energy is derived from the image in such a way that the snake is attracted to certain image features. Definitions of external energy are, amongst others, based on the image intensity, $I(x, y)$, or on the intensity of Gaussian smoothed images, $(G_\sigma(x, y) * I(x, y))$. However, in most snake-type techniques the intensity gradient is considered as the primary image feature, leading to the following external term:

$$E_{ext} = \oint_t -||\nabla I(x, y)||dt \quad (4)$$

where the gradient image $||\nabla I(x, y)||$ is usually derived from the intensity image through Gaussian smoothed derivatives.

The use of the gradient image only, however, neglects information that is available from the 2D gradient field, namely the vector direction. This problem is solved by Worring et al. [8]. They use the product of the normal to the active contour and the gradient vector of the object in order to distinguish between the object of interest and neighboring objects.

An other problem when using intensity gradient information is that intensity edges may appear in the scene without a material/color transition to support it. As a consequence, when using intensity edges as image features, the image segmentation results obtained by snakes may be negatively affected by the imaging-process (e.g. shadows, shading and highlights). Whereas in the traditional active contour methods the image intensity discontinuities are used to guide the deformation process, we focus on using color *invariant* information instead.

3 Color Invariant Snakes

Let the color gradient be denoted by $\nabla \mathcal{C}$, then the color-based external energy is as follows:

$$E_{ext} = \oint_t -||\nabla \mathcal{C}(x, y)||dt \quad (5)$$

Our aim is to analyze and evaluate different color models to produce robust color gradients ∇C discounting shadows, shading and highlights. To this end, in Section 3.1, we briefly discus various standard color models. In section 3.2, the dichromatic reflection model is presented. In Section 3.2.1 and 3.2.2, we discuss the theory that we have recently proposed on color invariant models, see [1] for example. Finally, various alternatives for ∇C are given in Section 3.3.

3.1 Color Models

In this paper, we concentrate on the following standard, color features derived from RGB: intensity $I(R,G,B) = R+B+G$, normalized colors $r(R,G,B) = \frac{R}{R+G+B}$, $g(R,G,B) = \frac{G}{R+G+B}$, $b(R,G,B) = \frac{B}{R+G+B}$, and hue $H(R,G,B) = \arctan\left(\frac{\sqrt{3}(G-B)}{(R-G)+(R-B)}\right)$.

3.2 The Reflection Model

Consider an image of an infinitesimal surface patch. Using the red, green and blue sensors with spectral sensitivities given by $f_R(\lambda)$, $f_G(\lambda)$ and $f_B(\lambda)$ respectively, to obtain an image of the surface patch illuminated by a SPD of the incident light denoted by $e(\lambda)$, the measured sensor values will be given by Shafer [5]:

$$C = m_b(\vec{n},\vec{s}) \int_\lambda f_C(\lambda)e(\lambda)c_b(\lambda)d\lambda + m_s(\vec{n},\vec{s},\vec{v}) \int_\lambda f_C(\lambda)e(\lambda)c_s(\lambda)d\lambda \qquad (6)$$

for $C = \{R,G,B\}$ giving the Cth sensor response. Further, $c_b(\lambda)$ and $c_s(\lambda)$ are the albedo and Fresnel reflectance respectively. λ denotes the wavelength, $\vec{n}$ is the surface patch normal, $\vec{s}$ is the direction of the illumination source, and $\vec{v}$ is the direction of the viewer. Geometric terms m_b and m_s denote the geometric dependencies on the body and surface reflection respectively.

Considering dichromatic reflectance and white illumination, then $e(\lambda) = e$ and $c_s(\lambda) = c_s$. The measured sensor values are then:

$$C_w = em_b(\vec{n},\vec{s})k_C + em_s(\vec{n},\vec{s},\vec{v})c_s \int_\lambda f_C(\lambda)d\lambda \qquad (7)$$

for $C_w \in \{R_w, G_w, B_w\}$ giving the red, green and blue sensor response under the assumption of a white light source. $k_C = \int_\lambda f_C(\lambda)c_b(\lambda)d\lambda$ is a compact formulation depending on the sensors and the surface albedo.

If the integrated white condition holds (i.e. for equi-energy white light the areas under the three curves are equal):

$$\int_\lambda f_R(\lambda)d\lambda = \int_\lambda f_G(\lambda)d\lambda = \int_\lambda f_B(\lambda)d\lambda = f \qquad (8)$$

we have:

$$C_w = em_b(\vec{n},\vec{s})k_C + em_s(\vec{n},\vec{s},\vec{v})c_s f \qquad (9)$$

3.2.1 Photometric invariant color features for matte, dull surfaces

Consider the body reflection term of eq. (9):

$$C_b = em_b(\vec{n},\vec{s})k_C \qquad (10)$$

for $C_b \in \{R_b, G_b, B_b\}$ giving the red, green and blue sensor response of a matte, dull surface patch under the assumption of a white light source.

According to the body reflection term, the color depends only on k_C (i.e. sensors and surface albedo) and the brightness on factor $em_b(\vec{n},\vec{s})$. As a consequence, a uniformly painted surface (i.e. with fixed k_C) may give rise to a broad variance of RGB values due to the varying circumstances induced by the image-forming process such as a change in object orientation, illumination intensity and position. The same argument holds for intensity I.

In contrast, normalized color rgb is insensitive to surface orientation, illumination direction and intensity as can be seen from:

$$r(R_b, G_b, B_b) = \frac{em_b(\vec{n}, \vec{s})k_R}{em_b(\vec{n}, \vec{s})(k_R + k_G + k_B)} = \frac{k_R}{k_R + k_G + k_B} \tag{11}$$

only dependent on the sensors and the surface albedo. Equal arguments hold for g and b.

Similarly, hue H is an invariant for matte, dull surfaces:

$$H(R_b, G_b, B_b) = \arctan\Big(\frac{\sqrt{3}em_b(\vec{n}, \vec{s})(k_G - k_B)}{em_b(\vec{n}, \vec{s})((k_R - k_G) + (k_R - k_B))}\Big) = \arctan\Big(\frac{\sqrt{3}(k_G - k_B)}{(k_R - k_G) + (k_R - k_B)}\Big) \tag{12}$$

In practice, the assumption of objects composed of matte, dull surfaces is not always realistic. To that end, the effect of surface reflection (highlights) is discussed in the following section.

3.2.2 Photometric invariant color features for both matte and shiny surfaces

Consider the surface reflection term of eq. (9):

$$C_s = em_s(\vec{n}, \vec{s}, \vec{v})f \tag{13}$$

for $C_s \in \{R_s, G_s, B_s\}$ giving the red, green and blue sensor response for a highlighted surface patch with white illumination.

Note that under the given conditions, the color of highlights is not related to the color of the surface on which they appear, but only on the color of the light source. Thus for the white light source, the surface reflection color cluster is on the diagonal grey axis of the basic RGB-color space corresponding to intensity I.

For a given point on a shiny surface, the contribution of the body reflection component C_b and surface reflection component C_s are added together $C_w = C_s + C_b$. Hence, the observed colors of the surface must be inside the triangular color cluster in the RGB-space formed by the two reflection components.

Because H is a function of the angle between the main diagonal and the color point in RGB-sensor space, all possible colors of the same (shiny) surface region (i.e. with fixed albedo) have to be of the same hue as follows from substituting eq. (9) in the hue equation:

$$H(R_w, G_w, G_w) = \arctan\Big(\frac{\sqrt{3}(G_w - B_w)}{(R_w - G_w) + (R_w - B_w)}\Big) =$$

$$\arctan\left(\frac{\sqrt{3}em_b(\vec{n}, \vec{s})(k_G - k_B)}{em_b(\vec{n}, \vec{s})((k_R - k_G) + (k_R - k_B))}\right) = \arctan\left(\frac{\sqrt{3}(k_G - k_B)}{(k_R - k_G) + (k_R - k_B)}\right) \tag{14}$$

factoring out dependencies on illumination e, object geometry $m_b(\vec{n}, \vec{s})$, viewpoint $m_s(\vec{n}, \vec{s}, \vec{v})$, and specular reflection coefficient c_s and hence only dependent on the sensors and the surface albedo. Note that $R_w = em_b(\vec{n}, \vec{s})k_R + em_s(\vec{n}, \vec{s}, \vec{v})c_s f$, $G_w = em_b(\vec{n}, \vec{s})k_G + em_s(\vec{n}, \vec{s}, \vec{v})c_s f$, and $B_w = em_b(\vec{n}, \vec{s})k_B + em_s(\vec{n}, \vec{s}, \vec{v})c_s f$.

Obviously other color features depend on the contribution of the surface reflection component and hence are sensitive to highlights.

3.3 Color Invariant Gradients

In the previous section, the effect of varying imaging circumstances have been studied for dichromatic reflectance under white illumination differentiated for intensity I, RGB, normalized color rgb, and hue H. According to eq. 5, we need to define the color gradient $\nabla\mathcal{C}(x, y)$ differentiated for the various color models.

3.3.1 Gradients in multi-valued images

In contrast to gradient methods which combine individual components of a multi-valued image in an ad hoc manner without any theoretical basis (e.g. taking the sum or RMS of the component gradient magnitudes as the magnitude of the resultant gradient), we follow the principled way to compute gradients in vector images as described by Silvano di Zenzo [6] and further used in [7], which is summarized as follows.

Let $\Theta(x_1, x_2) : \Re^2 \to \Re^m$ be a m-band image with components $\Theta_i(x_1, x_2) : \Re^2 \to \Re$ for $i = 1, 2, ..., m$. For color images we have $m = 3$. Hence, at a given image location the image value is a vector in $\Re^m$. The difference at two nearby points $P = (x_1^0, x_2^0)$ and $Q = (x_1^1, x_2^1)$ is given by $\triangle\Theta = \Theta(P) - \Theta(Q)$. Considering an infinitesmall displacement, the difference becomes the differential $d\Theta = \sum_{i=1}^{2} \frac{\partial\Theta}{\partial x_i} dx_i$ and its squared norm is given by:

$$d\Theta^2 = \sum_{i=1}^{2}\sum_{k=1}^{2} \frac{\partial\Theta}{\partial x_i}\frac{\partial\Theta}{\partial x_k} dx_i dx_k = \sum_{i=1}^{2}\sum_{k=1}^{2} g_{ik} dx_i dx_k = \begin{bmatrix} dx_1 \\ dx_2 \end{bmatrix}^T \begin{bmatrix} g_{11} & g_{12} \\ g_{21} & g_{22} \end{bmatrix} \begin{bmatrix} dx_1 \\ dx_2 \end{bmatrix} \tag{15}$$

where $g_{ik} := \frac{\partial\Theta}{\partial x_i} \cdot \frac{\partial\Theta}{\partial x_k}$ and the extrema of the quadratic form are obtained in the direction of the eigenvectors of the matrix $[g_{ik}]$ and the values at these locations correspond with the eigenvalues given by:

$$\lambda_\pm = \frac{g_{11} + g_{22} \pm \sqrt{(g_{11} - g_{22})^2 + 4g_{12}^2}}{2} \tag{16}$$

with corresponding eigenvectors given by $(\cos\theta_\pm, \sin\theta_\pm)$, where $\theta_+ = \frac{1}{2}\arctan\frac{2g_{12}}{g_{11} - g_{22}}$ and $\theta_- = \theta_+ + \frac{\pi}{2}$. Hence, the direction of the minimal and maximal changes at a given image location is expressed by the eigenvectors θ_- and θ_+ respectively, and the corresponding magnitude is given by the eigenvalues λ_- and λ_+ respectively. Note that λ_- may be different than zero and that the strength of an multi-valued edge should be expressed by how λ_+ compares to λ_-, for example by subtraction $\lambda_+ - \lambda_-$ as proposed by [7], which will be used to define gradients in multi-valued color *invariant* images in the next section.

3.3.2 Gradients in multi-valued color invariant images

In this section, we propose color invariant gradients based on the multi-band approach as described in the previous section.

The color gradient for RGB is as follows:

$$\nabla\mathcal{C}_{RGB} = \sqrt{\lambda_+^{RGB} - \lambda_-^{RGB}} \tag{17}$$

for

$$\lambda_{\pm} = \frac{g_{11}^{RGB} + g_{22}^{RGB} \pm \sqrt{(g_{11}^{RGB} - g_{22}^{RGB})^2 + 4(g_{12}^{RGB})^2}}{2} \tag{18}$$

where $g_{11}^{RGB} = |\frac{\partial R}{\partial x}|^2 + |\frac{\partial G}{\partial x}|^2 + |\frac{\partial B}{\partial x}|^2$, $g_{22}^{RGB} = |\frac{\partial R}{\partial y}|^2 + |\frac{\partial G}{\partial y}|^2 + |\frac{\partial B}{\partial y}|^2$, $g_{12}^{RGB} = \frac{\partial R}{\partial x}\frac{\partial R}{\partial y} + \frac{\partial G}{\partial x}\frac{\partial G}{\partial y} + \frac{\partial B}{\partial x}\frac{\partial B}{\partial y}$.

Similarly, we propose that the color invariant gradient for matte objects is given by:

$$\nabla \mathcal{C}_{rgb} = \sqrt{\lambda_{+}^{rgb} - \lambda_{-}^{rgb}} \tag{19}$$

for

$$\lambda_{\pm} = \frac{g_{11}^{rgb} + g_{22}^{rgb} \pm \sqrt{(g_{11}^{rgb} - g_{22}^{rgb})^2 + 4(g_{12}^{rgb})^2}}{2} \tag{20}$$

where $g_{11}^{rgb} = |\frac{\partial r}{\partial x}|^2 + |\frac{\partial g}{\partial x}|^2 + |\frac{\partial b}{\partial x}|^2$, $g_{22}^{rgb} = |\frac{\partial r}{\partial y}|^2 + |\frac{\partial g}{\partial y}|^2 + |\frac{\partial b}{\partial y}|^2$, $g_{12}^{rgb} = \frac{\partial r}{\partial x}\frac{\partial r}{\partial y} + \frac{\partial g}{\partial x}\frac{\partial g}{\partial y} + \frac{\partial b}{\partial x}\frac{\partial b}{\partial y}$.

Unlike the other color models, hue H is defined on a ring ranging $[0, 2\pi)$ instead of a linear *interval*. As a consequence, a low hue value (near 0) and a high hue value (near 2π) are positioned nearby on the ring. To cope with the wrap-around nature of hue, we define the difference between two hue values h_1 and h_2 as follows:

$$d(h_1, h_2) = \sqrt{(\cos h_1 - \cos h_2)^2 + (\sin h_1 - \sin h_2)^2} \tag{21}$$

yielding a difference $d(h_1, h_2) \in [0, 2]$ between h_1 and h_2.

Then the color invariant gradient for matte and shiny objects is given by:

$$\nabla \mathcal{C}_H = \nabla H \tag{22}$$

where standard edge detection is performed on the H by Canny's edge detection algorithm based on the the difference measure given by eq. (21).

Note that H varies with a change in material only, rgb with a change in material and highlights, and RGB vary with a change in material, highlights and geometry of an object. Based on these observation, we may conclude that $\nabla \mathcal{C}_{RGB}$ measures the presence of (1) shadow or geometry edges, (2) highlight edges, (3) material edges. Further, $\nabla \mathcal{C}_H$ measures the presence of (2) highlight edges, (3) material edges. And $\nabla \mathcal{C}_H$ measures the presence of only (3) material edges.

To evaluate the performance of the color snake differentiated for the various color gradient fields, the methods are compared, in the next section, on color images taken from full-color objects in real-world scenes.

4 Experiments

The objects considered during the experiments were recorded in 3 RGB-colors with the aid of the SONY XC-003P CCD color camera (3 chips) and the Matrox Magic Color frame grabber. The digitization was done in 8 bits per color. Two light sources of average daylight color were used to illuminate the objects in the scene. The size of the images are

128x128. In the experiments, the same weights have been used for the shape and image feature constraints.

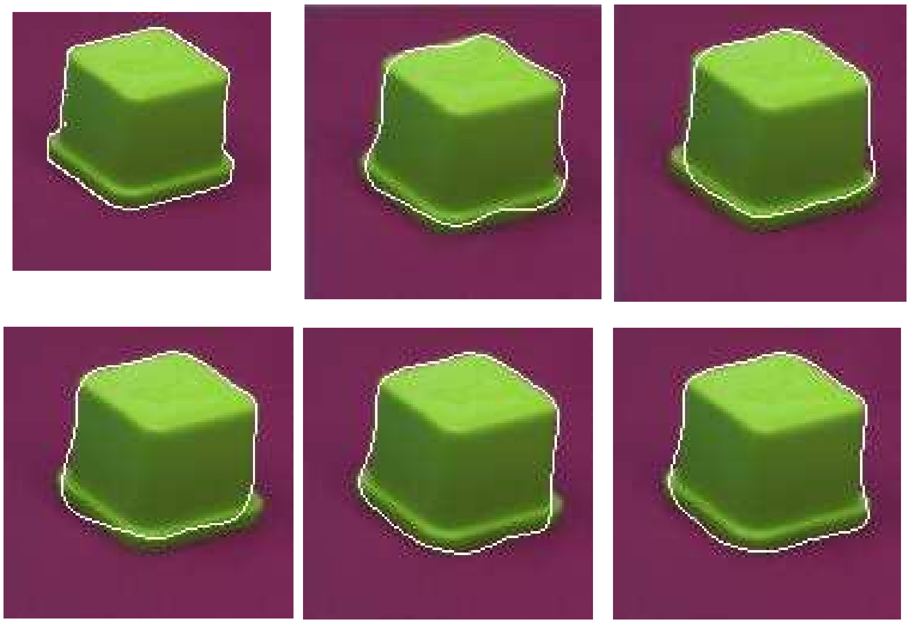

Figure 1: *From top left to right bottom a. Color image with ground-truth denoted by the white contour. b. The initial contour as specified by the user (the white contour). c. Snake segmentation result based on intensity gradient field ∇I. d. Snake segmentation result based on RGB gradient field $\nabla \mathcal{C}_{RGB}$. d. Snake segmentation result based on rgb gradient field $\nabla \mathcal{C}_{rgb}$. f. Snake segmentation result based on H gradient field $\nabla \mathcal{C}_H$.*

Figure 1.a shows the image of a matte cube against a homogeneous background. The ground-truth (the true boundary) is given by the white contour. The image is clearly contaminated by shadows, shading and minor highlights. Note that the cube is painted homogeneously. Further, in Figure 1.b, the initial contour is shown as specified by the user (the white contour). As one can see, the snake segmentation results based on intensity I gradient denoted by ∇I and the RGB color gradient denoted by $\nabla \mathcal{C}_{RGB}$ are negatively affected by shadows and shading due to the varying shape of the object. In fact, for these gradient fields is not clear to which boundaries the snake contour should be pulled to. As a consequence, the final contour is biased and poorly defined. In contrast, the final contours obtained by the snake method based on $\nabla \mathcal{C}_{rgb}$ and $\nabla \mathcal{C}_H$ gradient information, are nicely pulled towards the true boundary and hence correspond neatly with the material transition.

Figure 2 shows an image of a red highlighted ball and a matte cube. Further, in Figure 3, an image is shown containing two specular plastic donuts on top of each other. Again the images are affected by shadows, shading, highlights and inter-reflections. Inter-reflections occur when an object receives the reflected light from other objects. Note that each individual object is painted homogeneously with a distinct color. The snake segmentation results based on intensity I and color RGB gradient are poorly defined due to the disturb-

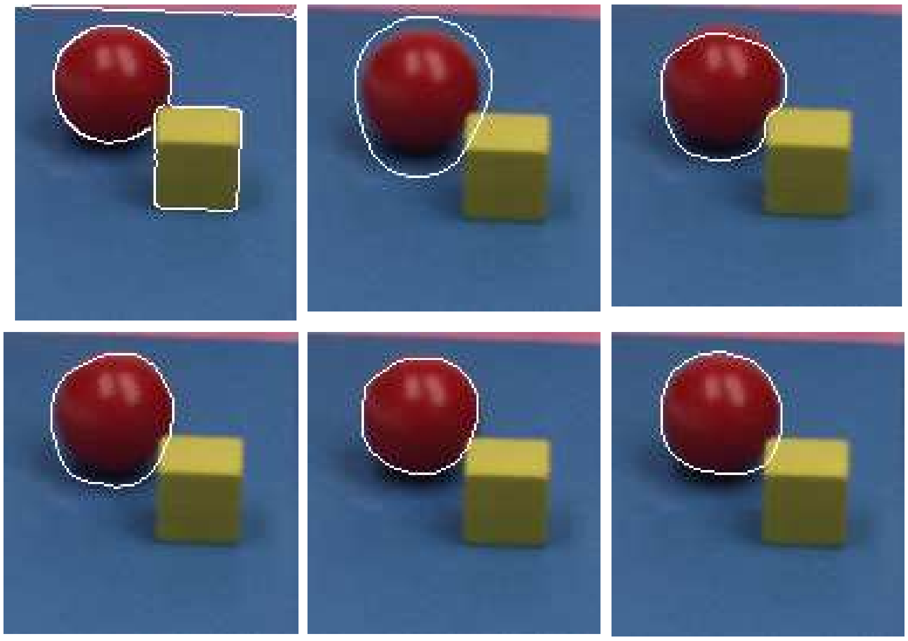

Figure 2: *From top left to right bottom a. Color image with ground-truth denoted by the white contour. b. The initial contour as specified by the user (the white contour). c. Snake segmentation result based on intensity gradient field* ∇I. *d. Snake segmentation result based on* RGB *gradient field* $\nabla \mathcal{C}_{RGB}$. *e. Snake segmentation result based on* rgb *gradient field* $\nabla \mathcal{C}_{rgb}$. *f. Snake segmentation result based on* H *gradient field* $\nabla \mathcal{C}_H$.

ing influences of the imaging conditions (mostly due to the shadows around the objects). The final contours obtained by the snake method based on $\nabla \mathcal{C}_{rgb}$ and $\nabla \mathcal{C}_H$ gradient information, are nicely pulled towards the true edge and hence correspond again nicely to the material transition. Note that in Figure 3.f the initial contour has been partly converged to the wrong boundary. This an inherent problem of snakes in general where initial contour must, in general, be close to the true boundary or else it will likely converge to the wrong boundary. For color snakes, this can be solved by taking the color at both sides of a hue transition into account.

5 Conclusion

In this paper, we have proposed the use of color *invariant* gradient information to guide the deformation process to obtain snake boundaries which correspond to material boundaries in images discounting the disturbing influences of surface orientation, illumination, shadows and highlights.

Experimental results show that the proposed color invariant snake successfully find material contours discounting other ”accidental” edges types (e.g. shadows and highlight transitions). Comparison with intensity-based snakes shows that the intensity-based snake

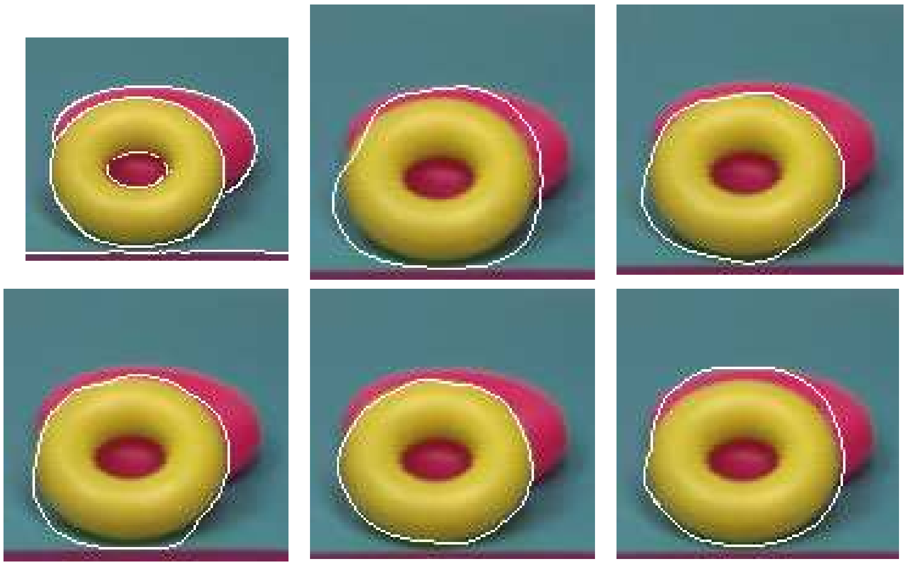

Figure 3: *From top left to right bottom a. Color image and ground-truth given by the white contour. b. The initial contour as specified by the user (the white contour). c. Snake segmentation result based on intensity gradient field* ∇I. *d. Snake segmentation result based on* RGB *gradient field* $\nabla \mathcal{C}_{RGB}$. *e. Snake segmentation result based on* rgb *gradient field* $\nabla \mathcal{C}_{rgb}$. *f. Snake segmentation result based on* H *gradient field* $\nabla \mathcal{C}_H$.

is dramatically outperformed by the presented color invariant snake.

No constraints have been imposed on the images and the camera imaging process other than that images should be taken from colored objects illuminated by average day-light color. It is our point of view that these conditions are acceptable for a large variety of applications.

References

[1] Gevers, T. and Smeulders, A. W. M., *Image Indexing using Composite Color and Shape Invariant Features*, ICCV, Bombay, India (1998)

[2] Bajcsy, R., Lee S. W., and Leonardis, A., *Color Image Segmentation with Detection of Highlights and Local Illumination Induced by Inter-reflections*, In IEEE 10th ICPR'90, pp. 785-790, Atlantic City, NJ, 1990.

[3] Klinker, G. J., Shafer, A. and Kanada, T., *A Physical Approach to Color Image Understanding,* Int. J. of Comp. Vision, Vol. 4, pp. 7-38, 1990.

[4] M. Kass, A. Witkin, D. Terzopoulos, *Snakes: Active Contour Models,* International Journal of Computer Vision, 1(4), pp. 321-331, 1988.

[5] Shafer, S. A., *Using Color to Separate Reflection Components,* COLOR Res. Appl., 10(4), pp 210-218, 1985.

[6] S. di Zenzo, *Gradient of a Multi-images,* CVGIP, 33:116-125, 1986.

[7] G. Sapiro, D. L. Ringach, *Anisotropic Diffusion of Multi-valued Images with Applications,* to Color Filtering, IEEE PAMI, (5)11, 1582-1586, 1996.

[8] M. Worring, A. W. M. Smeulders, L.H. Staib, J.S. Duncan, *Parameterized feasible boundaries in gradient vector fields,* Information Processing in Medical Imaging, 48-61, 1993.